

Assessing cellular automata based models using partial differential equations

Andrea Doeschl, Matt Davison, Henning Rasmussen
and Greg Reid

Department of Applied Mathematics
University of Western Ontario
London, Ontario, Canada, N6A 5B7

Abstract

This paper presents a novel method for assessing cellular automata based models. The cellular model considered in this paper was designed to simulate sediment transport and topographic changes in rivers. It will be demonstrated how prior knowledge about partial differential equations and their solution schemes can be used to provide deeper insight into the performance of two numerical implementations for this cellular model. This research takes part in an ongoing discussion about reductionist (models that reduce the system to its fundamental laws) and cellular approaches (models that strive to capture the relevant qualitative features of a system without the detail of the reductionist approach) to model complex natural behavior. This study links the two approaches and should contribute to a better understanding of the advantages of each approach.

Keywords: Cellular automata, Numerical models of fluvial processes, Partial differential equations

1 Introduction

Mathematical and numerical models have become a common tool for studying complex natural phenomena. Traditional modeling approaches aim to identify the governing mechanical processes and represent them by systems of integro- and partial differential equations. In most cases, these can only be solved numerically. Good numerical approximations of the solutions of the system often require formidable numerical skills and extensive computer power. This reductionist modeling approach has proved greatly successful in simulating the behavior of many complex systems. Simultaneously, the formulation and assessment of numerical solution schemes has become an extensive research field. However, the detailed representation of the governing physical processes associated with the reductionist approach often requires in addition to considerable computing time, excellent skills not only for programming but also for interpretation of the detailed results.

During the last few decades, cellular automata models have emerged as an alternative modeling approach [1]. Instead of reducing the system to its fundamental components, cellular automata models focus on key aspects of the system and use simple rules to represent them quantitatively. Rather than reproducing the detailed behavior of a system, cellular automata based models aim to capture its relevant characteristics. Cellular automata portray the system by discrete sets of cells which interact with each other according to simple rules which represent the system's mechanics in a highly simplified manner. This discrete, simplistic representation certainly lacks the microscopic fidelity of reductionist models, but opens many new possibilities for exploring the system's behavior. In systems with complicated boundary conditions or domain geometry, cellular models can be much faster than reductionist models [2]. Further, simple cellular models can often be constructed without the extensive human time involved in constructing and solving models based on differential equations. Interpretation of the results of a cellular model are facilitated by the limited focus on some aspects of the system.

Both modeling approaches have obvious advantages and have contributed to a better understanding of many natural and artificial systems. However, both approaches also demand a high price for their advantages. Reductionist models often obscure the fundamental aspects that control the overall behavior of the modelled system. Further, they reach their limits when the underlying physical principles of the phenomenon are unknown or when sys-

tems become too complex to solve by analytical or numerical means. Cellular models, which concentrate on key aspects of the modelled system, are generally difficult to validate. The assessment of these models is often restricted to visualization of the results and lacks rigorous analysis. To enhance the recognition of the key aspects and to relieve the burden of lengthy computations, many reductionist models depicted by complex systems of partial differential equations have been simplified to cellular automata [3]. The question arises, whether insights obtained from the traditional reductionist modeling approach can also help towards a more rigorous assessment of cellular models. The aim of this paper is to demonstrate how partial differential equations can be used to assess numerical schemes arising from a mathematical cellular automata model.

The present studies focus on a cellular model for sediment transport and topographic changes in river beds. The model was generated to examine the essential criteria for the establishment and propagation of braided channel patterns in rivers [4] and has found further applications for studying the impact of environmental change in catchment areas [5] and the role of vegetation for bank stability [6]. Due to the simplified representation of the governing processes, the model has provoked intense debates in the fluvial community [6]. Whereas many are attracted by the powerful results in return for simple, fast computations, others are skeptical about the validity of the model predictions. This scepticism is grounded in the difficulty in validating the numerical results, which are supposed to capture the characteristic behavior of the system instead of simulating its behavior in great detail. The present studies help to fill this gap.

For the purpose of this study it is convenient to reduce the original two dimensional model to one dimension. In one dimension, the model predicts the evolution of a longitudinal river profile through the propagation of water and sediment. Two rival numerical implementations for the model will be presented, provoking questions about the advantages of each approach and about the model's robustness to different numerical implementations. These questions are tackled by deriving partial differential equations which correspond to both implementations and by assessing the numerical implementations as solution schemes of the corresponding equations. Depending on the parameter choice, the model can be linear or non-linear. The investigations start with the linear model ($m = 1$), for which a variety of rigorous assessment methods for numerical solution schemes can be applied, and continue with the more realistic non-linear phenomenon, ($m \neq 1$).

2 The cellular model in one dimension

Obviously, models of braided river processes require at least two spatial dimensions, and the advantages of the cellular automata approach over the reductionist approach can only be evident in two or higher dimensions. Nevertheless, for the purpose of this study, reduction of the problem to one dimension not only facilitates the problem but also provides deeper insight into the cellular model and its numerical implementations.

In one dimension, the model mimics the following simple process: starting with a longitudinal initial profile of a riverbed, water and sediment introduced at the upstream end propagate in the downstream direction. The propagation of sediment causes erosion and deposition at different locations, which changes the bed profile (Figure 1).

The cellular model divides the bed profile into a sequence of discrete cells of equal length Δx . Each cell of the 1D lattice has coordinates (x, y) , where x is the location of the cell center and y is the average bed elevation in the cell length. The model variables are the water flux Q and the sediment flux M . The propagation of water and sediment is discretized by transferring both quantities from cell to cell. The propagation of water follows the principle of conservation of mass, implying that the water which enters a cell also leaves the cell during the same time step. In one dimension this implies a constant water flux Q . The sediment transport between adjacent cells obeys the following rule, deduced from empirical studies [7], [4]:

$$M = \begin{cases} K(QS)^m & \text{if } S \leq 0 \\ 0 & \text{if } S > 0 \end{cases}$$

The parameter K in the above equation is an unconstrained scaling constant and the exponent m is positive. The variable S is the slope between adjacent cells. Empirical studies suggest values between $m = \frac{5}{3}$ and $m = 2.5$ ([7], [8]). Since, in 1D, Q is constant, the above equation simplifies to

$$M = \begin{cases} \tilde{K}S^m & \text{if } S \geq 0 \\ 0 & \text{if } S < 0 \end{cases} \quad (1)$$

The cell elevation change Δy during a time step obeys the mass balance equation

$$\Delta y = M_{in} - M_{out},$$

where M_{in} and M_{out} denote the amounts of sediment entering and leaving the cell respectively.

3 Two rival numerical implementations

Many mathematical models offer different numerical implementations which represent the physics of the problem from different perspectives. Alternative numerical implementations are good for evaluating the schemes and testing the model's robustness. For fluvial processes, the main rival numerical implementations are the Eulerian and the Lagrangian approach. The Eulerian approach describes the state of the system at fixed points in space and calculates subsequent states by synchronous updates of all mesh points. The Lagrangian method employs a moving frame of reference and describes the state of the system by particles that move with respect to each other [9].

The cellular model described in Section 2 lends itself to two different numerical implementations: the Eulerian approach and a method that compromises between the Eulerian and the Lagrangian approach.

In the Eulerian approach, which operates on a fixed lattice, the amounts of water and sediment in each cell at time $k\Delta t$ are calculated from the corresponding amounts at the previous time $(k-1)\Delta t$ and the incoming and out-flowing quantities during that time interval. If M^k is the quantity of a material in a cell at time $k\Delta t$ and $M_{in}^{(k,k+1)}$ and $M_{out}^{(k,k+1)}$ are the quantities entering and leaving the cell during the time interval $[k\Delta t, (k+1)\Delta t]$ respectively, then the quantity M at time $(k+1)\Delta t$ is given by

$$M^{k+1} = M^k + M_{in}^{(k,k+1)} - M_{out}^{(k,k+1)}. \quad (2)$$

In this Eulerian approach, all grid cells are simultaneously updated during an iteration, so that one iteration corresponds to one time step $[k\Delta t, (k+1)\Delta t]$. The output after k iterations is the topography at time $k\Delta t$.

The second approach, which we call the Marker-in-cell (MIC) method, also uses a fixed lattice and mixes aspects of the Eulerian and Lagrangian implementations. Instead of looking at the evolution of the entire lattice simultaneously, one moves with the quantities as they propagate along the lattice. One starts at the first lattice cell and updates the cell quantities as one propagates in the downstream direction. We call the sequence of water and sediment distribution from the first to the last lattice column one *sweep*.

In contrast to one iteration in the Eulerian method, one sweep is associated with several time steps. The material transfer between the first and second cells happens before the material transfer between consecutive cells. The MIC method provides direct answers to questions concerning the effects of events at one location on further downstream locations. Estimates of the bed profile at a given time $k\Delta t$ can however also be calculated. Using the same notation as in equation (2), the quantity M in a cell changes twice during one sweep and satisfies the following system of equations:

$$\begin{aligned} M^{k+1} &= M^k + M_{in}^{(k,k+1)}, \\ M^{k+2} &= M^{k+1} - M_{out}^{(k+1,k+2)}, \end{aligned} \tag{3}$$

where M^{k+2} denotes the quantity M at the end of the sweep and the superscripts $(k, k + 1)$ and $(k + 1, k + 2)$ correspond to the time intervals $[k\Delta t, (k + 1)\Delta t]$ and $[(k + 1)\Delta t, (k + 2)\Delta t]$ respectively.

The most essential difference between both modeling approaches is the immediate update of cell elevations in the MIC method. This affects the local slopes and consequently the amounts of transferred sediment between adjacent cells. These discrepancies may cause essential differences in the model predictions and provokes the suspicion that the mathematical cellular model may not be robust to different numerical implementations. If this is the case, which numerical model produces more realistic results?

Figure 2 shows time snapshots of a river bed profile represented by a one dimensional lattice of six cells, predicted by the Eulerian (left) and MIC approach (right). In this computational experiment, the Eulerian approach calculates a different profile at a given time than the MIC approach (dashed lines). However, both methods predict the same asymptotic behavior (solid lines). Various computational experiments for longer one dimensional lattices and for different sized two dimensional lattices all performed with a variety of parameter choices indicate that both approaches predict generally similar long-term behaviors, as shown in [10]. The aim of the present study is to support the observations from the numerical experiments by a more rigorous mathematical analysis.

4 Derivation of partial differential equations from both numerical schemes

4.1 Partial differential equation associated with the Eulerian approach

Let $y_i^n = y(i\Delta x, n\Delta t)$ denote the elevation of cell i at time $t_n = n\Delta t$, where Δx and Δt are the cell length and the time step in the numerical models. Taking cell dimension and time into account, the mass balance equation is

$$\frac{y_i^{n+1} - y_i^n}{\Delta t} \Delta x = K \left[H(-S_i^n) (-S_i^n)^m - H(-S_{i+1}^n) (-S_{i+1}^n)^m \right], \quad (4)$$

where

$$S_i^n = \frac{y_{i-1}^n - y_i^n}{\Delta x}$$

and $H(x)$ is the Heaviside step function, one if $x \geq 0$ and zero for $x < 0$. In the following we will assume that the slopes S_i^n and S_{i+1}^n are always negative so that $H = 1$. If this is not the case, equation 4 does not yield a partial differential equation and modifications of the function H are required. We defer a discussion of the resulting complications to the concluding section of this paper.

Using truncated Taylor series expansions and taking the limits $\Delta x \rightarrow 0$ and $\Delta t \rightarrow 0$, equation 4 yields under the assumption $H = 1$ the differential equation

$$\frac{\partial y}{\partial t} - Km \left(-\frac{\partial y}{\partial x} \right)^{m-1} \frac{\partial^2 y}{\partial x^2} = 0. \quad (5)$$

Equation (5) is a diffusion equation with diffusion coefficient $Km(-y_x)^{m-1}$. The Eulerian approach is known as the explicit difference scheme for solving the diffusion equation [11].

4.2 Partial differential equation associated with the Marker-in-cell method

The MIC-method involves three time levels during one sweep. Using the same notation as above, the mass-balance equation for cell i can be expressed as

$$\frac{y_i^{n+2} - y_i^n}{2\Delta t} \Delta x = K \left[H(-S_i) (-S_i)^m - H(-S_{i+1}^{n+1}) (-S_{i+1}^{n+1})^m \right]. \quad (6)$$

The terms in the above equation can be expanded into truncated Taylor series expansions at the mesh point $(i\Delta x, (n+1)\Delta t)$. Assuming $H = 1$ as above as well as finite $v = \frac{\Delta x}{\Delta t}$ yields, after taking the limits $\Delta t \rightarrow 0$, $\Delta x \rightarrow 0$ the differential equation

$$\frac{\partial y}{\partial t} = Km \left(-\frac{\partial y}{\partial x} \right)^{m-1} \frac{\partial^2 y}{\partial x^2} + \frac{Km}{v} \left(-\frac{\partial y}{\partial x} \right)^{m-1} \frac{\partial^2 y}{\partial x \partial t}. \quad (7)$$

In the following we set $v = 1$ without loss of generality.

The first term on the right-hand side is the same diffusion term as obtained from the Euler method. The propagation of sediment, an explicit component in the cellular MIC method, results in the additional mixed derivative term in the MIC-partial differential equation. Understanding and interpreting the difference between the cellular Eulerian and MIC approach therefore reduces to the question: how does the additional term on the right-hand side of equation (7) affect the solutions of the corresponding initial-value problem. This term transforms the parabolic diffusion equation into a hyperbolic equation. Both parabolic and hyperbolic equations, describe evolution processes, but hyperbolic equations are generally associated with the propagation of waves or signals ([12]). Mathematically, the two equation classes require different solution techniques and lead to solutions with different qualitative behaviors.

In contrast to the Eulerian method, which is the well-known forward Euler method for solving the diffusion equation, the MIC-method cannot be identified as a familiar numerical solution scheme for approximating the solution of equation (7).

5 Analyzing the linear PDEs and their solutions

For $m = 1$, the differential equations (5) and (7) are linear and analytic solutions can be obtained for appropriate initial and boundary conditions. The solution of the linear diffusion problem

$$\begin{aligned}\frac{\partial y}{\partial t} &= K \frac{\partial^2 y}{\partial x^2} \\ y(x, 0) &= y_0(x)\end{aligned}\tag{8}$$

with an integrable real function y_0 is

$$y(x, t) = \frac{1}{\sqrt{4\pi Kt}} \int_{-\infty}^{\infty} y_0(u) e^{-\frac{(x-u)^2}{4Kt}} du.\tag{9}$$

Hyperbolic linear second order partial differential equations generally require two initial conditions for a unique solution. However, a unique solution can be obtained for the following initial-boundary value problem that uses one initial condition and a weak boundary condition at infinity [13]

$$\begin{aligned}\frac{\partial y}{\partial t} &= K \left(\frac{\partial^2 y}{\partial x^2} + \frac{\partial^2 y}{\partial x \partial t} \right) && \text{for } x \in \mathfrak{R}, t > 0, \\ y(x, 0) &= y_0(x) && \text{for } x \in \mathfrak{R}, \\ \lim_{|x| \rightarrow \infty} |y(x, t)| &< \infty && \text{for } t \geq 0\end{aligned}\tag{10}$$

for a continuous, differentiable, bounded real-valued function y_0 [13]. The solution of (8)

$$y(x, t) = \int_{-\infty}^t g(x-u) e^{\frac{u-2t}{K}} I_0 \left(\frac{2}{K} \sqrt{t(t-u)} \right) du,\tag{11}$$

where

$$g(x) = \frac{1}{K} y_0(x) - y_0'(x)$$

and I_0 is the modified Bessel function of the first kind of order 0.

At first glance, the analytical solutions (9) and (11) of the linear diffusion and MIC equations do not appear similar. For example, for fixed times $t > 0$ the solution of the linear diffusion equation is an even function in x provided the initial function $y_0(x)$ is even. In contrast, the solution of the MIC equation involves the integration over the interval $(-\infty, t]$ indicating a non-symmetrical temporal evolution of an even initial function. The suspicion arises that the great similarity in the numerical predictions observed in the computational experiments is not captured by the analytical solutions of the corresponding 1D problems. Analytical comparison between the exact solutions of systems (8) and (10) with the same initial function however reject this suspicion. We have shown in [13], that the exact solutions of both systems rapidly converge to each other as time increases. Further, for

finite times and bounded initial functions with bounded first derivatives, the discrepancy between both solutions is also bounded.

Figure 3 shows time snapshots of the analytic solutions (left) of the initial value problems (8) and (10) and of the corresponding difference function $e(x, t)$ (right) for different initial functions y_0 . The analytical solutions greatly resemble one another and the magnitude of the difference function decreases as time increases. The mixed derivative term in the MIC equation can be identified as a process that inhibits the symmetric evolution of the initial function, which is controlled by the diffusion process. But compared to the diffusion process, this inhibiting process is very weak. The study of the MIC equation revealed that the hyperbolic MIC equation shares some properties with parabolic equations. This observation is interesting in its own right and is therefore covered in a separate paper. We refer the interested reader to [13].

5.1 Assessment of the linear numerical Eulerian and MIC schemes

The quality of finite difference schemes for approximating solutions of partial differential equations is determined by the following four criteria: accuracy of the numerical solutions, consistency and convergence of the schemes and stability [11]. For constant coefficient linear finite difference schemes, methods to assess the validity of all four criteria are well established. In particular, the explicit (Eulerian) method as solution scheme of the linear diffusion initial-value problem can be found in any standard textbook (e.g. [11]) and is summarized in Table 1. . Substitution of the exact solution of the linear MIC equation into the finite difference equation 6 yields the local truncation errors and the result for consistency for the MIC scheme, as presented in Table 5.1. Lax-Richtmyer's definition of stability [11] yields that the linear MIC scheme is unstable and hence not convergent. Nevertheless, applying von Neumann's Fourier-series method, it can be shown that the amplification rate of the round-off errors is small (i.e. for $\frac{K\Delta t}{(\Delta x)} < \frac{1}{2}$, the stability condition for the linear explicit scheme, round-off errors grow at a rate less than $\sqrt{5}$), suggesting that the MIC model is valid for a limited time interval (Figure 4).

<i>Criterion / Scheme</i>	<i>Local truncation error</i>	<i>Consistent</i>	<i>Convergent</i>	<i>Stable</i>
Euler	$O(\Delta t) + O(\Delta x^2)$	yes	yes	if $\frac{K\Delta t}{(\Delta x)^2} < 0.5$
MIC	$O(\Delta t) + O(\Delta x^2)$	yes	no	no, but bounded growth of errors

Table 1: Evaluation of the linear numerical difference schemes according to four criteria.

6 Analyzing the non-linear PDEs and their numerical solutions

Most natural phenomena represent non-linear relationships between interacting components. In particular, if the components are water and sediment flux, an exaggerated response of sediment to water flux is crucial for topographic changes in many rivers [6]. For $m > 1$, the partial differential equations (5) and (7) cannot be solved analytically and most methods devised to assess the linear solution schemes are inapplicable. The quality of the non-linear Eulerian and MIC schemes will be assessed in comparison to other numerical solution schemes of the corresponding partial differential equations. Although the analysis of the non-linear numerical schemes is less rigorous than the analysis of the linear counterparts, an insight into model behaviors is nevertheless obtained.

6.1 Numerical solutions of the non-linear diffusion initial-value problem

An alternative numerical solution of the non-linear initial-value problem

$$\frac{\partial y}{\partial t} = Km \left(-\frac{\partial y}{\partial x} \right)^{m-1} \frac{\partial^2 y}{\partial x^2}, \quad (12)$$

$$y(x, 0) = y_0(x), \quad (13)$$

with $m \neq 1$ can be obtained using similarity transformations [14]. The above system has stretching symmetry provided

$$y_0(\lambda x) = g(\lambda)y_0(x) \quad (14)$$

for every real constant λ and a real function g . In particular, functions of the form

$$y_0(x) = Ax^a$$

satisfy the above condition. The restriction to a finite domain or additional boundary conditions would however break the stretching symmetry. The stretching symmetry of the initial value problem (12, 13) yields similarity transformations of the system's variables, which transform the initial value problem into an ordinary differential equation boundary-value problem. As the transformation depends on the initial values, we restrict the assessment to two specific examples where the initial function $y_0(x) = y(x, 0)$ satisfies condition (14). For the purpose of this study we consider the following initial conditions:

$$y(x, 0) = \begin{cases} k_1x & \text{for } x < 0 \\ k_2x & \text{for } x \geq 0 \end{cases} \quad (15)$$

and

$$z(x, 0) = \begin{cases} A\sqrt{-x} & \text{for } x < 0 \\ -A\sqrt{x} & \text{for } x \geq 0 \end{cases} \quad (16)$$

where k_1 and k_2 are negative constants and A is a positive constant. The transformations

$$\begin{aligned} r &= t^{-\frac{1}{2}}x \\ Y(r) &= t^{-\frac{1}{2}}y(x, t) \end{aligned}$$

and

$$\begin{aligned} r &= t^{-\frac{1}{2}}x \\ U(r) &= u(x, t), \end{aligned}$$

where $u(x, t) = \frac{\partial u}{\partial x}(x, t)$ yield, after substitution into equations (12, 15) the system of first order ordinary differential equations

$$\begin{aligned} Y' &= U \\ U' &= \frac{Y-rU}{2Km(-U)^{m-1}} \end{aligned} \quad (17)$$

with boundary conditions

$$\begin{aligned} Y(-\infty) &= \infty & U(-\infty) &= -k_1 \\ Y(\infty) &= -\infty & U(\infty) &= k_2. \end{aligned} \quad (18)$$

Instead of the partial differential equation (12) with initial conditions (15) we now have to solve the first order system of ordinary differential equations (17) with boundary conditions (18). The problem with using $\pm\infty$ as boundary points can be overcome by using the shooting method ([15]), for which constants $Z_0 = Z(0)$ and $U_0 = U(0)$ are sought that yield the correct behavior of U and Z at $\pm\infty$.

The same techniques applied to the initial value problem (12, 16), see [10], give rise to the similarity transformations

$$\begin{aligned} r &= t^{-\frac{2}{m+3}}x \\ Z(r) &= t^{-\frac{1}{m+3}}z(x, t) \\ Y(r) &= |r|^{-\frac{1}{2}}Z(r) \end{aligned}$$

and yield, after substitution the second-order ordinary differential equation

$$\frac{2}{m+3}|r|^{\frac{2}{3}}Y'(r) + KM \left(\left(-\sqrt{|r|}Y(r) \right)' \right)^{m-1} \left(\sqrt{|r|}Y(r) \right)^{m''} = 0 \quad (19)$$

with constant boundary conditions

$$\begin{aligned} \lim_{r \rightarrow -\infty} Y(r) &= A \\ \lim_{r \rightarrow \infty} Y(r) &= -A. \end{aligned} \quad (20)$$

6.2 Numerical solutions of the non-linear MIC initial-value problem

The MIC initial value problem

$$\frac{\partial y}{\partial t} = Km \left(-\frac{\partial y}{\partial x} \right)^{m-1} \left(\frac{\partial^2 y}{\partial x^2} + \frac{\partial^2 y}{\partial x \partial t} \right) \quad (21)$$

$$y(x, 0) = y_0(x) \quad (22)$$

also has the stretching symmetry for particular initial functions. However, the resulting differential equation contains singularities, which disable the application of the shooting method to estimate starting points for the numerical schemes. For this reason we aimed to construct a finite difference scheme that satisfies the same initial and boundary conditions as the MIC method. These criteria hold for an implicit scheme that uses forward difference approximations for the derivatives y_t and y_x respectively and a central difference approximation for y_{xx} . The mixed derivative y_{xt} at the (i, n) th mesh-point is approximated by

$$\frac{\partial^2 y}{\partial x \partial t} \Big|_{(i,n)} \sim \frac{1}{\Delta x \Delta t} \left(y_i^{n+1} - y_i^n - y_{i-1}^{n+1} + y_{i-1}^n \right).$$

In contrast to the above similarity solutions, the implicit scheme operates like the MIC and Eulerian scheme on finite domains. For specified values at the boundaries $x = 0$, $x = L$ and $t = 0$, the implicit scheme calculates the values of the interior mesh-points via

$$L(y_i^n, y_{i+1}^n) y_i^{n+1} = R(y_{i-1}^n, y_i^n, y_{i+1}^n, y_{i-1}^{n+1}),$$

where L and R are the non-linear functions

$$\begin{aligned} L &= 1 - \frac{Km}{\Delta x} \left(\frac{y_i^n - y_{i+1}^n}{\Delta x} \right)^{m-1} \\ R &= y_i^n + \frac{Km\Delta t}{(\Delta x)^2} \left(\frac{y_i^n - y_{i+1}^n}{\Delta x} \right)^{m-1} \left(y_{i-1}^n - 2y_i^n + y_{i+1}^n \right) \\ &\quad + \frac{Km}{\Delta x} \left(\frac{y_i^n - y_{i+1}^n}{\Delta x} \right)^{m-1} \left(y_{i-1}^n - y_i^n - y_{i-1}^{n+1} \right). \end{aligned}$$

6.3 Numerical Results

Calculations of the numerical solutions

Numerical similarity solutions to solve the boundary value problems (17, 18) and (19), (20) were obtained by the solution method *dverk78* - a seventh to eighth order Runge-Kutta method ([16]) in the software package MAPLE 6. Amongst the variety of numerical solvers incorporated into MAPLE 6, *dverk78* presented the best compromise between calculation time and error tolerance. The presented numerical results correspond to an error tolerance $< 10^{-8}$. The constants k_1 , k_2 and A in the above examples were chosen such that the constants themselves and the truncated values of the

solutions at the starting point $r = 0$, which were estimated by the shooting method, comprised at most three digits, when an accuracy of seven decimal places was used.

The Eulerian method operates on a finite spatial domain. To allow comparison with the numerical similarity solutions, the influence of the domain boundaries for the explicit (Eulerian) method was minimized by calculating the solutions for a large spatial domain (i.e. $x \in [-500, 500]$) without fixing the elevations at the boundaries. The comparison with the approximated similarity solutions was then performed for a relatively small range of x values (i.e. $x \in [-10, 10]$) far away from the boundaries. For the comparison of the three finite difference schemes, the initial conditions (15) and (16) were modified to the following set of initial-boundary conditions

$$y(x, 0) = \begin{cases} k_1 x & \text{for } -10 \leq x < 0 \\ k_2 x & \text{for } 0 \leq x \leq 10 \end{cases} \quad (23)$$

$$\begin{aligned} y(-L, t) &= k_1 L \\ y(L, T) &= -k_2 L \end{aligned} \quad (24)$$

and

$$y(x, 0) = \begin{cases} A\sqrt{-x} & \text{for } -10 \leq x < 0 \\ -A\sqrt{x} & \text{for } 0 \leq x \leq 10 \end{cases} \quad (25)$$

$$\begin{aligned} y(-L, t) &= A\sqrt{L} \\ y(L, T) &= -A\sqrt{L} \end{aligned} \quad (26)$$

with the same constants k_1 , k_2 and A as in equations (15) and (16). Instead of fixed boundary values, we could have also used zero or constant flux conditions at the boundaries of the spatial domain.

Comparison of the numerical results

Time snapshots of the approximate solutions to the non-linear diffusion and MIC problems for the above initial conditions are shown in Figures 5 and 6. Each of the numerical schemes we used predicted the evolution of the initial topographies towards a straight line. However, while the time snapshots corresponding to the numerical similarity solutions and the solutions of the explicit scheme are indistinguishable, a significant discrepancy between the solutions of the MIC scheme and the implicit scheme can be detected.

Accuracy of the numerical schemes

The local truncation errors of the finite difference schemes are

$$T_i^n = \begin{cases} O(\Delta t) + O(\Delta x^2) & \text{(Euler)} \\ O(\Delta t) + O(\Delta x^2) & \text{(MIC)} \\ O(\Delta t) + O(\Delta x) & \text{(Implicit)} \end{cases}$$

implying that the explicit method is more accurate than the MIC method and that the latter is more accurate than the implicit scheme. To compare these accuracies with the accuracy of the similarity solutions, a discrepancy function $D(t)$ between the solutions \hat{y} and \tilde{y} of two numerical schemes was defined by

$$D(t) = \max_{i \in I} \{ |\hat{y}(x_i, t) - \tilde{y}(x_i, t)| \},$$

where I denotes the set of x -values for which both solutions were obtained. Figure 7 shows that for $\Delta x = \Delta t = 0.5$, the maximal discrepancy between the solutions of the Eulerian and the similarity method at fixed t -values has order 10^{-2} for values of t between 0 and 500 and x in $[-10, 10]$ (top left graph). The discrepancy is surprisingly small considering the variety of errors introduced by the shooting method and the numerical solver in MAPLE in the numerical similarity solutions as well as the local truncation error of the Eulerian solution. The maximal discrepancies between the finite difference solutions, in particular between the solutions of the implicit scheme and the cellular schemes, are significantly higher (Figure 7).

Stability and Convergence

How stable are the non-linear Eulerian and MIC schemes compared to their linear counterparts and compared to other numerical solution schemes? Since rigorous general methods for assessing the stability of non-linear solution schemes do not exist [17], the above question was tackled by empirical means. These rely on the observation that the symptom of instability of the finite difference schemes are oscillations with temporally increasing amplitudes. Using fixed step sizes $\Delta x = \Delta t = 0.5$ for the finite difference schemes and varying exponent m , the smallest value of the scaling constant K was computed, for which oscillations occurred within 10,000 time steps. Under the assumption that the absence of oscillations indicates stability of the finite difference schemes, the following observations were made (Figure 7):

- Stability depends in part on the initial conditions.

- For all difference schemes, stability decreases with increasing exponent m . This implies instability for the non-linear MIC scheme and at most a conditional stability for the non-linear Eulerian scheme with stricter conditions than for the linear Eulerian scheme. The separation line between the stable and unstable region satisfies the inverse logarithmic relationship

$$\log_{10}(K) \propto \frac{1}{m}.$$

- The Eulerian method is always more stable than the MIC method. For relatively small m (i.e. $m \leq 2.5$ in Figure 7), both the MIC and Eulerian method are more stable than the implicit method. For larger m , the contrary is true.

Instability of the Runge-Kutta scheme used to derive the similarity solutions does not manifest itself in oscillating solutions. Although for some values of m and K in the unstable region of the Eulerian method, starting points $(Y(0), U(0))$ yielding the appropriate boundary conditions could not be obtained, numerical experiments indicate that the Runge-Kutta method devised for the similarity solutions is more stable than the other presented schemes.

The convergence of the Runge-Kutta scheme [18] and the good agreement between the solutions of the non-linear Eulerian and Runge-Kutta schemes in the common stability region suggests that the non-linear Eulerian scheme is also convergent when stable. Since the linear MIC scheme is not convergent, we deduce that the non-linear MIC method is also not convergent.

7 Discussion and Conclusions

The main goal of this study was to demonstrate how partial differential equations can be used to assess numerical models arising from a cellular automata approach. The study focused on two rival numerical models for morphological processes in river beds and addressed the following questions: How do both models differ in their predictions and what are the advantages of either approach? Can these simple numerical models compete with more sophisticated numerical schemes that model the same processes?

The relationship between the numerical cellular automata based models and partial differential equations was established by viewing the models as numerical solution schemes of partial differential equations with initial and boundary values derived from the governing equations of the cellular models. This viewpoint revealed that both models, when reduced to one dimension, have a strong diffusive component. The difference between the models consists of an additional expression in the MIC partial differential equation, represented by a second-order mixed derivative term. Understanding the difference between both numerical models boiled down to understanding the impact of this additional term in the MIC equation.

The foundations of this study were laid by analyzing the linear equations and solution procedures ($m = 1$) using a variety of established techniques. We could prove that the exact solutions of both problems are very similar and eventually converge. This implies that the additional, mixed derivative term in the MIC equation has negligible influence on the model predictions and is in good agreement with the observations from numerical experiments. In particular, it demonstrates that the linear cellular automata based model is robust to different numerical implementations. Computational experiments suggest that these results are also valid for the non-linear models in one and two dimensions. Further, we could show that the Eulerian method for solving the linear diffusion initial-value problem is more accurate and more stable than the MIC method for solving the MIC initial-boundary value problem. The combined results of the rigorous linear and the more empirical non-linear analysis suggest that the Eulerian approach is somewhat better than the MIC approach for modeling the temporal evolution of a longitudinal river profile. However, although the MIC method is less accurate and less stable, it produces good results for a limited time with sufficiently small time steps. The MIC model is therefore a valid approach for modeling phenomena that cannot be captured by the Eulerian approach. Such phenomena include the impact of upstream events on downstream regions.

Comparison with other numerical schemes for solving the corresponding non-linear partial differential equations shed light onto the advantages of both cellular models. As an alternative to the Eulerian model for solving the non-linear diffusion initial-value problem, the similarity method was combined with sophisticated numerical ODE solvers. Although these procedures appear more stable and may generate solutions of greater accuracy, their application is restricted to certain initial and boundary conditions. The Eulerian model, in contrast, generates solutions which differ little from those of

the more sophisticated scheme, but can be applied to a wide range of initial and boundary conditions. To solve the non-linear MIC equation we developed an implicit scheme that satisfies the same initial and boundary conditions as the MIC scheme. The implicit scheme required comparable computational effort to the explicit Eulerian and MIC schemes, but was trumped by the latter in accuracy and, for $m < 2.5$, also in stability. In summary, for the one dimensional initial and initial-boundary value problems, for which alternative numerical models could be applied, the cellular models performed well.

The fact that the cellular models are valid schemes to model simple processes, motivates us to consider applying these models to more complicated, higher dimensional problems. However, since the original cellular models of this study were two dimensional and applied to all initial topographies, it would be desirable to extend the present analysis to two dimensions and to lift the restriction to exclusively negative slopes. The latter could be achieved by replacing the Heaviside step functions in equations (4) and (6) by the differentiable function

$$H(x) = \frac{1}{2}(1 + \tanh(ax)),$$

where the constant a determines the slope of the curve near $x = 0$. The resulting, more complicated, differential equations apply for all local slopes and approximate the derived diffusion and MIC equation when a is large. Deriving partial differential equations from the two dimensional numerical models is also possible, but involves the consideration of water and sediment transport and the inclusion of six instead of two neighbors. In contrast to the one dimensional cellular automata based model, discharge is no longer constant in two dimensions, but depends on the local slopes, so that the models relate to systems of differential equations instead of one differential equation. The additional inclusion of more cell neighbors yields more terms in the mass balance equations. The differential equations resulting from these extensions are therefore significantly more complicated than the one dimensional initial value problems considered in this study and are not likely to serve as a means to gain insights into the cellular models. They rather confirm the advantage of the cellular approach as a tool to model processes that are difficult to model by other means.

References

- [1] Wolfram, S 2002. *A New Kind of Science* Wolfram Media, US.
- [2] McArdell, B., Faeh, R. 2000. *A computational investigation of river braiding*. Gravel-bed rivers 5. Hydrological Society Inc. Wellington.
- [3] Ermentrout, G. B. and Edelstein-Keshet, L. 1993. *Cellular automata approaches to biological modeling*. J. Theor. Biol. 160, 97-133.
- [4] Murray, A.B., Paola, C. 1994. *A cellular model of braided rivers*. Nature, 371, 54-57.
- [5] Coulthard, T.J., Kirkby, M.J. and Macklin, G.M. 1999. *Modelling the impacts of the holocene environmental change in an upland river catchment, using a cellular automaton approach*. Fluvial Processes and Environmental Change. Wiley, New York.
- [6] Paola, C. 2000. *Modelling stream braiding over a range of scales*. Gravel-bed rivers 5. Hydrological Society Inc. Wellington.
- [7] Engelund, F. and Hansen, E. 1967. *A monograph of sediment transport in alluvial streams*. Teknisk Forlag, Copenhagen.
- [8] Ashmore, P. 1985. *Process and form in gravel braided streams: Laboratory modelling and field observations*. PhD Thesis, University of Alberta, Edmonton.
- [9] Tetzlaff, D.M. and Harbaugh, J.W 1989. *Simulating clastic sedimentation*. Van Norstrand Reinhold, New York.
- [10] Doeschl, A. 2002. *Assessing braided river dynamics with a cellular model*. PhD Thesis, University of Western Ontario, London.
- [11] Smith, G.D. 1985. *Numerical solution of partial differential equations: finite difference methods*. Oxford Applied Mathematics and Computing Science Series, Third Edition, Oxford University Press, Oxford.
- [12] Logan, J.D. 1998. *An Introduction to nonlinear partial differential equations*. Wiley, New York.
- [13] Davison, M. and Doeschl, A. *Submitted 2002. A hyperbolic PDE with parabolic behaviour*.

- [14] Dresner, L. 1983. *Similarity solutions of non-linear partial differential equations*. Springer-Verlag, New York.
- [15] Johnson, L.W., Riess, R.D. 1982. *Numerical Analysis*. Addison-Wesley, Reading , chapter 7.8.2
- [16] Enright W.H. 1991. *The relative efficiency of alternative defect control schemes for high order continuous Runge-Kutta formulas*. Department of Computer Science, University of Toronto, Technical report 252/91.
- [17] Ames, W.F. 1992. *Numerical methods for partial differential equations*. Academic Press, New York.
- [18] Cartwright, J.H.E. and Oreste, P. 1992. *The dynamics of Runge-Kutta methods*. Int. J. Bifurcation and Chaos, 2, 427-449.

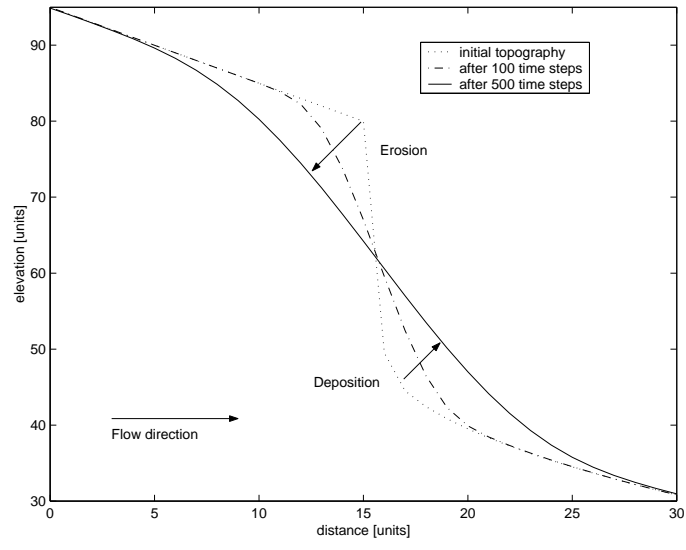


Figure 1: Schematic diagram of the temporal evolution of a river bed profile.

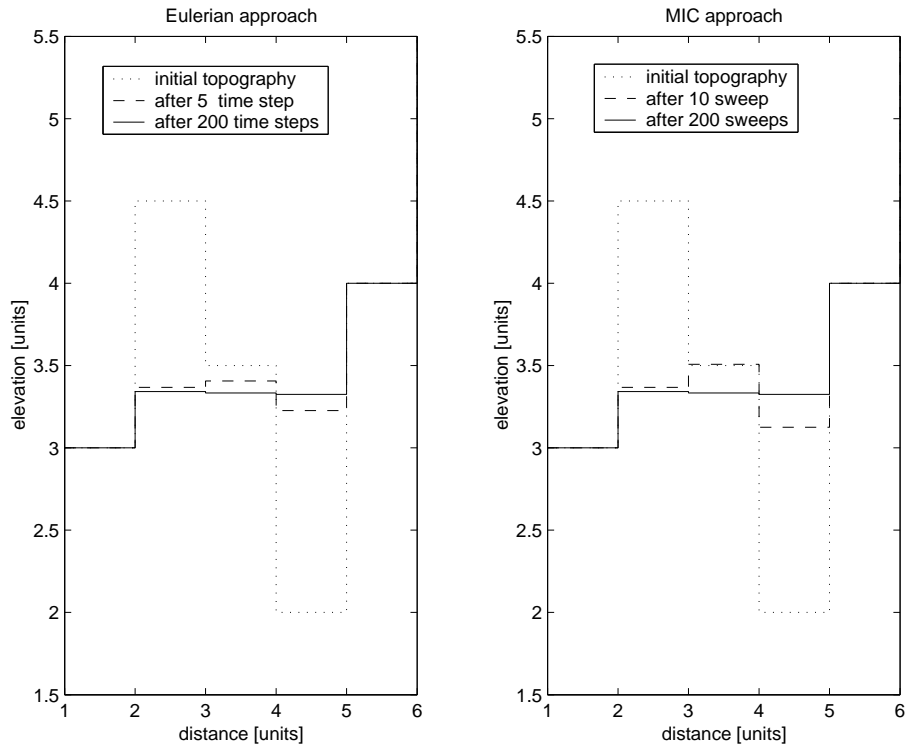


Figure 2: Time snapshots of the bed profile predicted by the Eulerian (left) and MIC method (right). The parameters used in this experiments were $K = 0.1$ and $m = 2$.

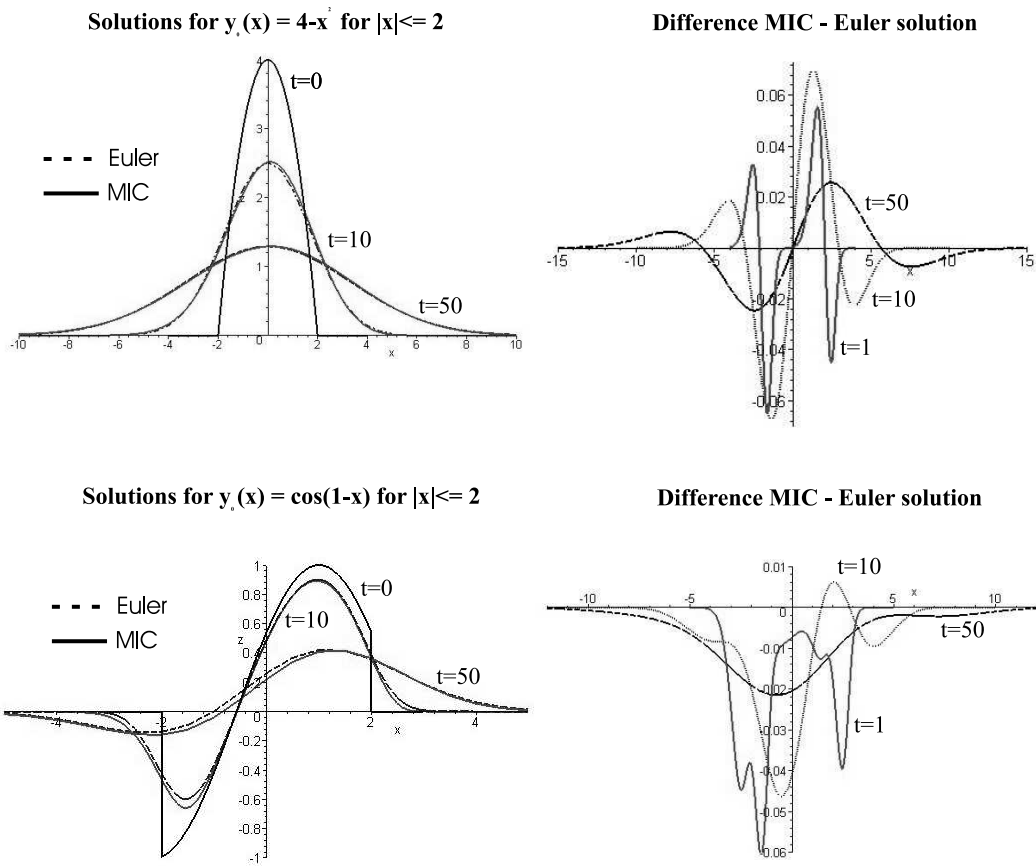


Figure 3: Time snapshots of the solutions for the MIC and Euler equation for different initial functions (left) and of their differences (right).

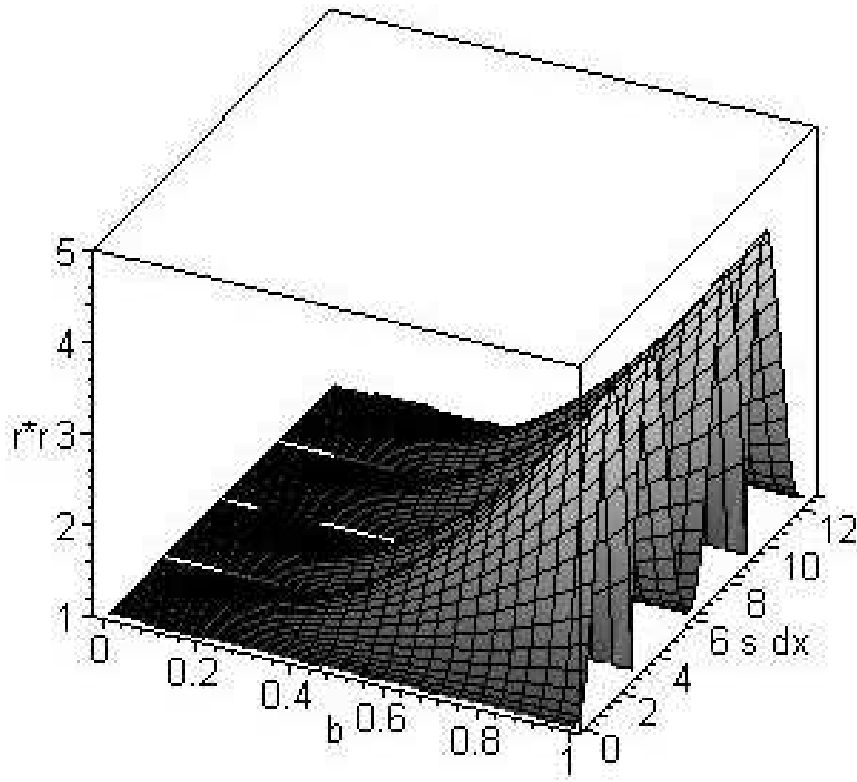


Figure 4: Amplification factor r^2 of the round-off errors in the MIC model as function of $b = \frac{K\Delta t}{(\Delta x)^2}$ and $s\Delta x$, where $s = \frac{\pi}{N\Delta x}$.

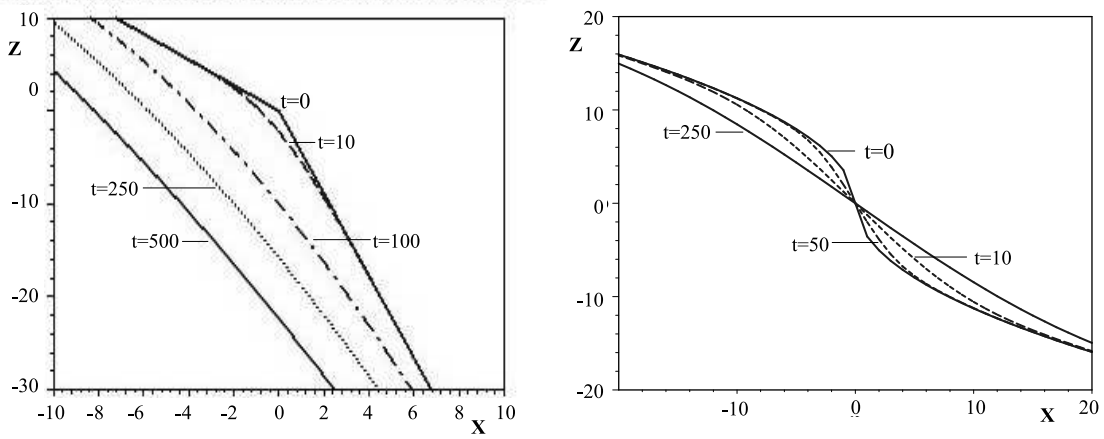


Figure 5: Time snapshots of the approximate solutions of the non-linear diffusion equation with initial function (15) (left) and (16) (right) for step sizes $\Delta x = \Delta t = 0.5$. The constants are $m = \frac{5}{3}$, $k_1 = -1.4$, $k_2 = -4.5$ and $K = 0.01$ (left) and $A = 3.56$ and $K = 0.1$ (right).

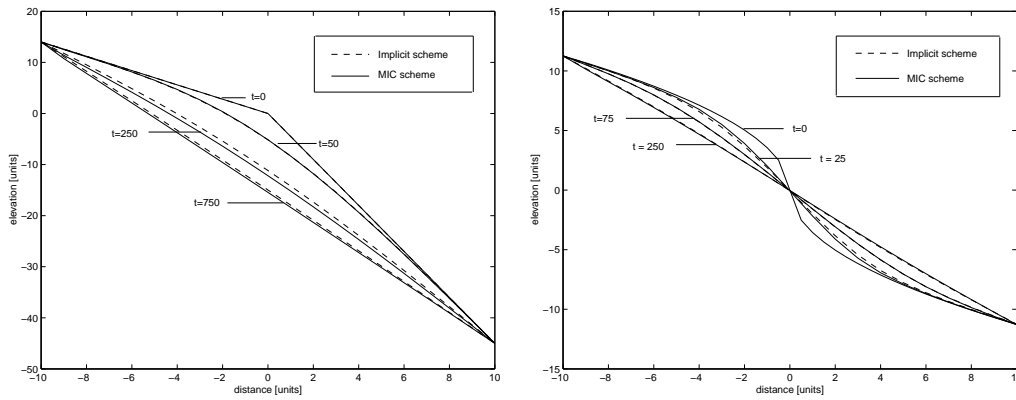


Figure 6: Time snapshots of the approximate solutions of the non-linear PDE (7) with initial-boundary conditions (23, 24) (left) and (25, 26) (right). The step sizes and constants were the same as used to generate Figure 5.

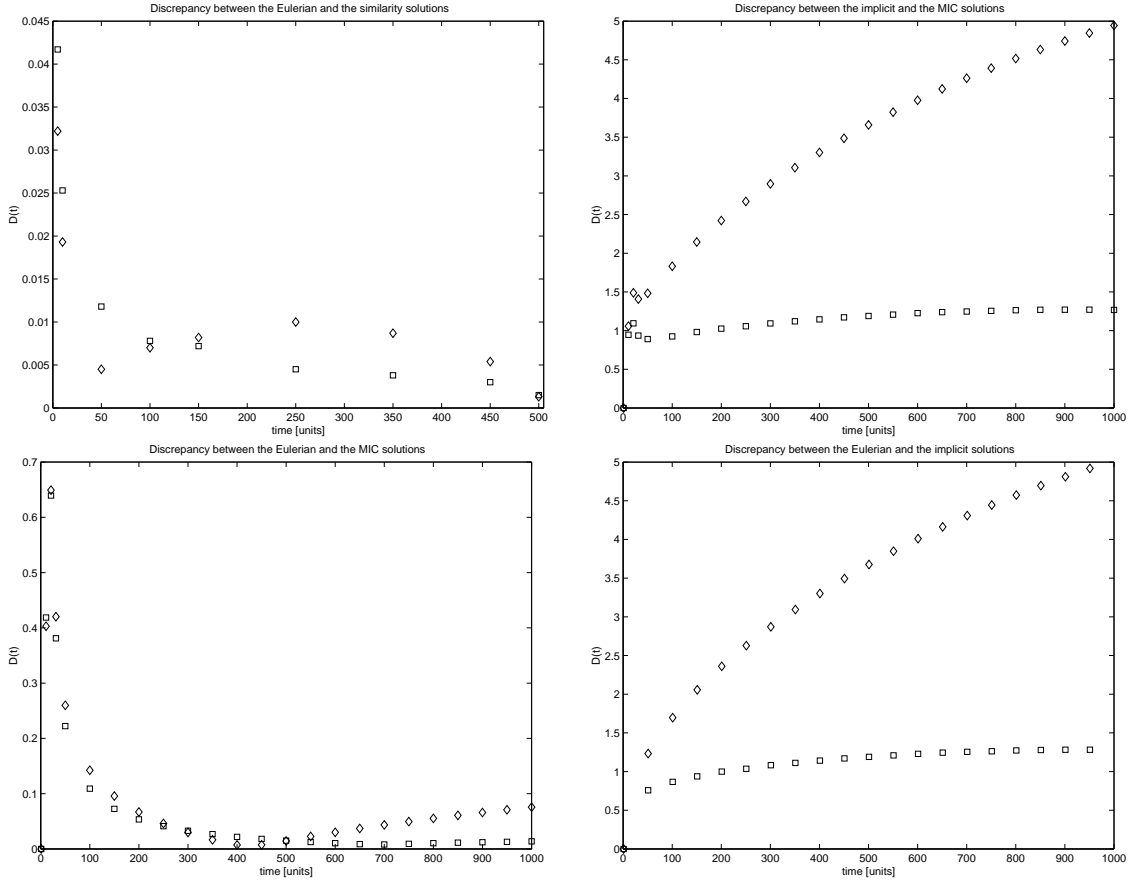


Figure 7: Maximal discrepancies between the solutions of different schemes. Diamonds refer to initial conditions (15) for the top left graph and (23) for the remaining graphs, respectively. Squares refer to the initial conditions (16) and (25) respectively. All runs used the same step sizes $\Delta x = \Delta t = 0.5$ and constants $K = 0.01$ and $m = \frac{5}{3}$.

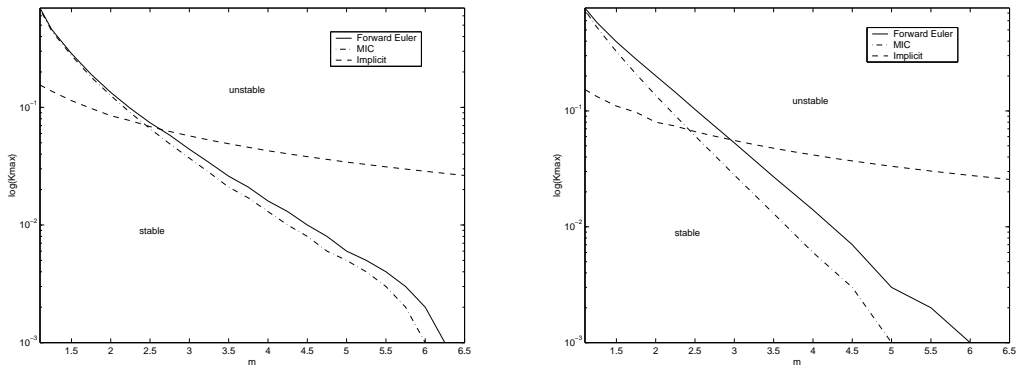


Figure 8: Relationship between the constants m and K for stability of the non-linear Eulerian, MIC and implicit schemes. The left figure refers to initial conditions (23, 24), the right figure refers to initial conditions (25, 26).